Electronic Supplementary Material (ESI) for Journal of Materials Chemistry C.

Supporting Information

Manipulation of Cl/Br Transmutation in Zero-Dimensional Mn^{2+}-Based Metal Halides toward Tunable Photoluminescence and Thermal Quenching Behaviors

Guojun Zhou[a], Zhiyang Liu[b], Maxim S. Molokeev[cde], Zewen Xiao[b], Zhiguo Xia[f] and Xian-Ming Zhang[*a]

[a] Key Laboratory of Magnetic Molecules and Magnetic Information Materials (Ministry of Education), School of Chemistry and Material Science, Shanxi Normal University, Linfen 041004, China. Email: zhangxm@dns.sxnu.edu.cn; Tel: +86-357-2051402

[b] Wuhan National Laboratory for Optoelectronics, Huazhong University of Science and Technology, Wuhan 430074, China

[c] Laboratory of Crystal Physics, Kirensky Institute of Physics, Federal Research Center KSC SB RAS, Krasnoyarsk 660036, Russia

[d] Siberian Federal University, Krasnoyarsk 660041, Russia

[e] Department of Physics, Far Eastern State Transport University, Khabarovsk 680021, Russia

[f] State Key Laboratory of Luminescent Materials and Devices and Institute of Optical Communication Materials, South China University of Technology, Guangzhou 510641, China

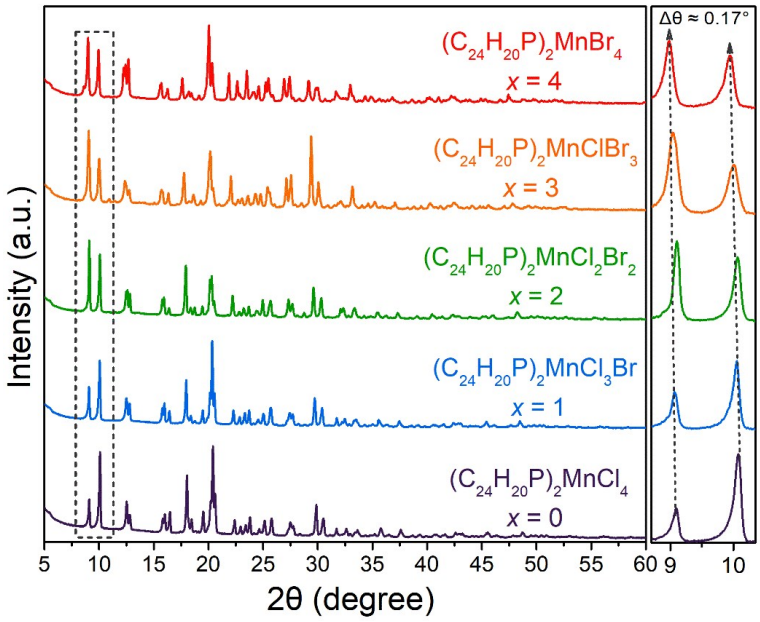

Figure S1. PXRD patterns of $(C_{24}H_{20}P)_2MnCl_{4-x}Br_x$ (x = 0, 1, 2, 3, 4) and the characteristic peaks which gradually shift to lower angles with the replacement of Cl atoms by Br.

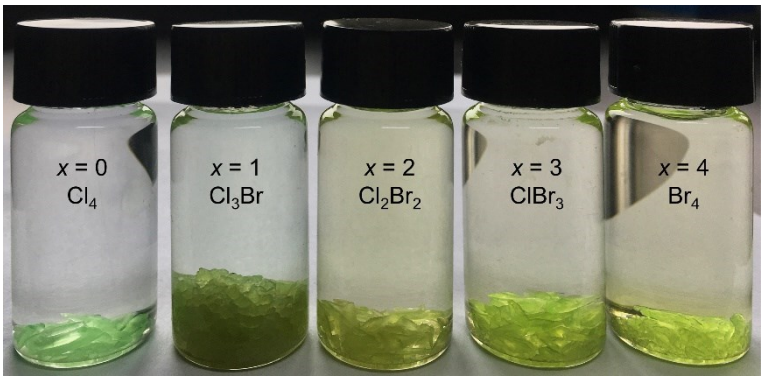

Figure S2. Photographs of $(C_{24}H_{20}P)_2MnCl_{4-x}Br_x$ (x = 0, 1, 2, 3, 4) single crystals under daylight.

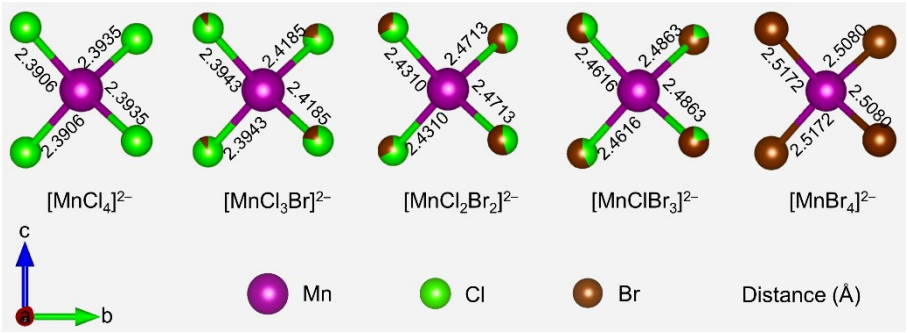

Figure S3. Local structures of $[MnX_4]^{2-}$ (X = Cl/Br) with different bond lengths.

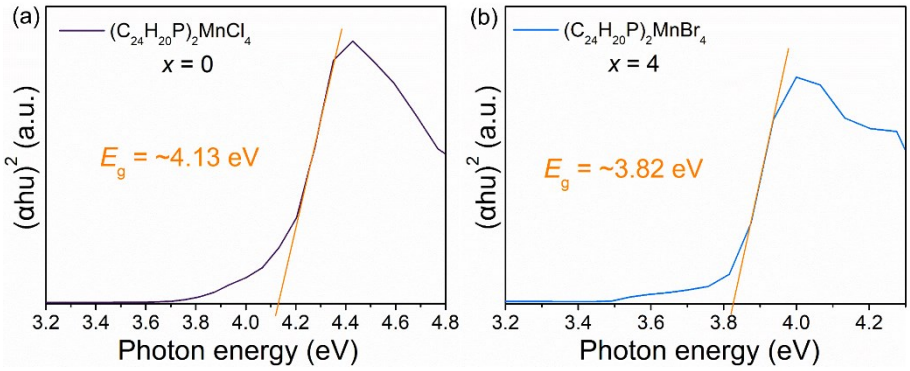

Figure S4. The extrapolations of band gap energy of (a) $(C_{24}H_{20}P)_2MnCl_4$ and (b) $(C_{24}H_{20}P)_2MnBr_4$.

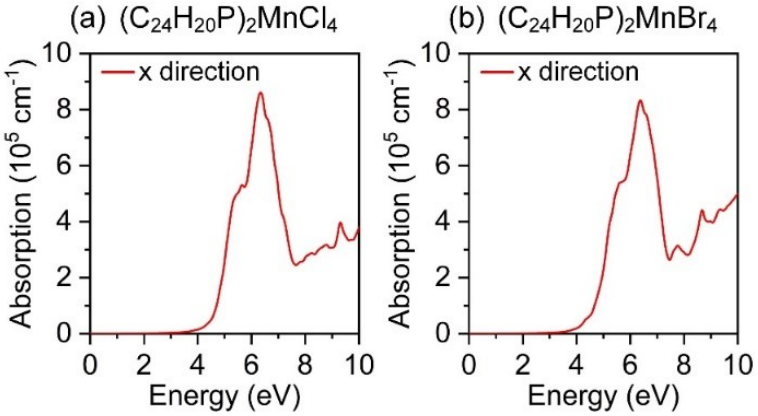

Figure S5. Optical absorption spectra of (a) $(C_{24}H_{20}P)_2MnCl_4$ and (b) $(C_{24}H_{20}P)_2MnBr_4$ calculated based on the HSE functional.

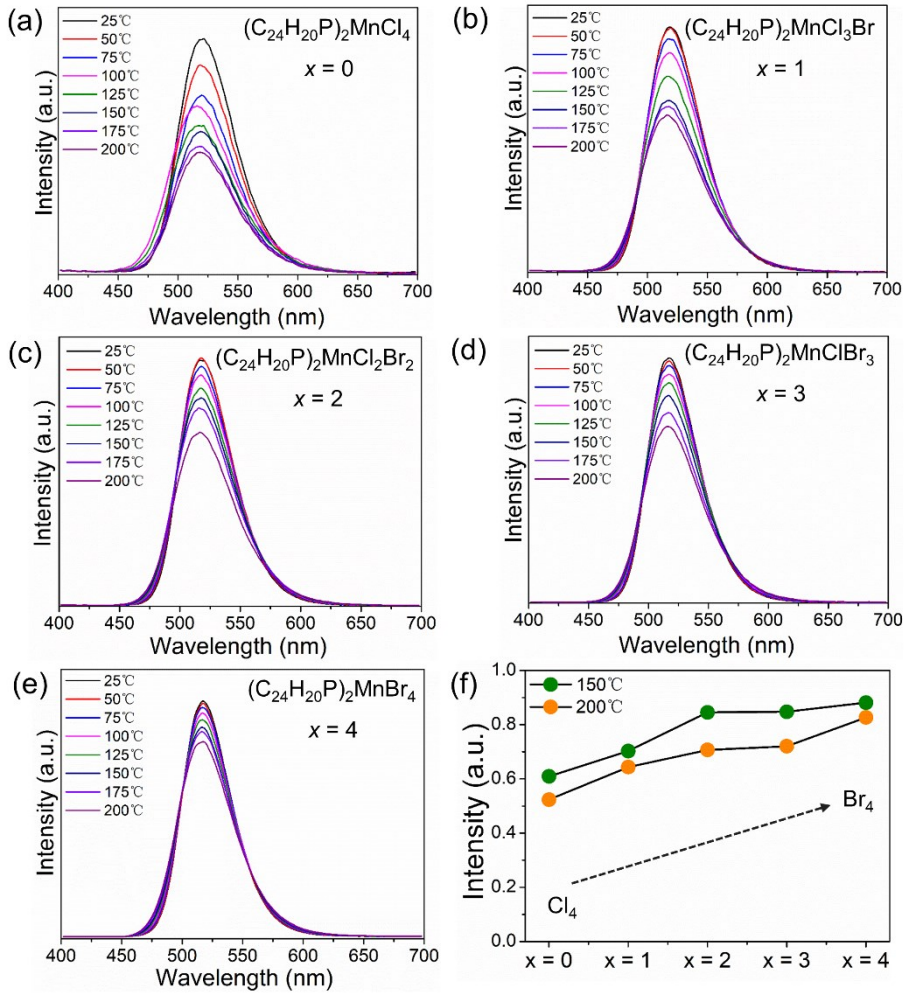

Figure S6 (a–e) Temperature-dependent PL spectra of $(C_{24}H_{20}P)_2MnCl_{4-x}Br_x$ (x = 0, 1, 2, 3, 4) under 365 nm excitation in the temperature range of RT–200 °C with an interval of 25 °C. (f) The thermal quenching trends of $(C_{24}H_{20}P)_2MnCl_{4-x}Br_x$ (x = 0, 1, 2, 3, 4) at 150 ℃ and 200 ℃, respectively.

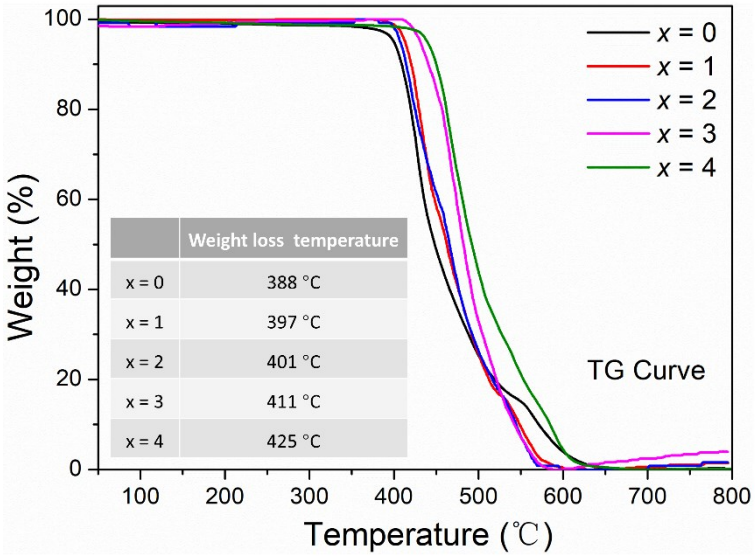

Figure. S7 Thermogravimetric (TG) curves of $(C_{24}H_{20}P)_2MnCl_{4-x}Br_x$ (x = 0, 1, 2, 3, 4).

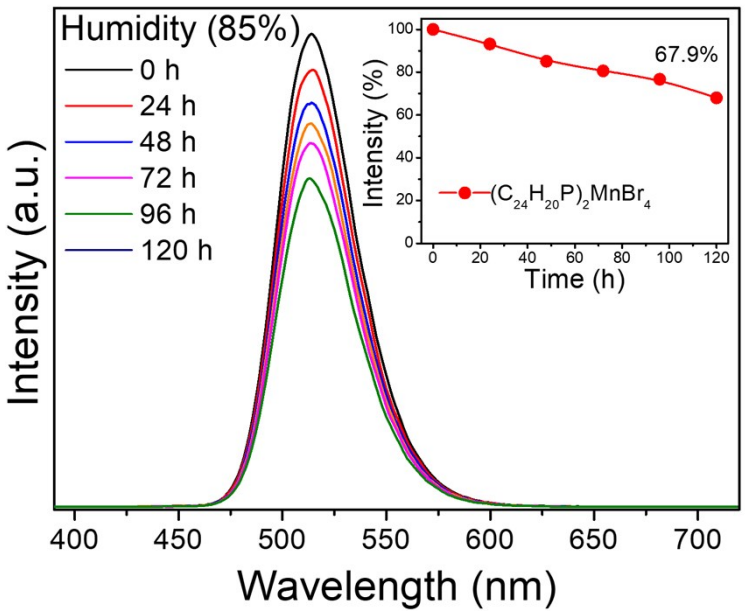

Figure. S8 Time-dependent PL spectra of $(C_{24}H_{20}P)_2MnBr_4$ at 85% humidity environment under 365 nm excitation in the time range of 0–120 h with a time interval of 24 h, and the inset is a changing trend of emission intensity.

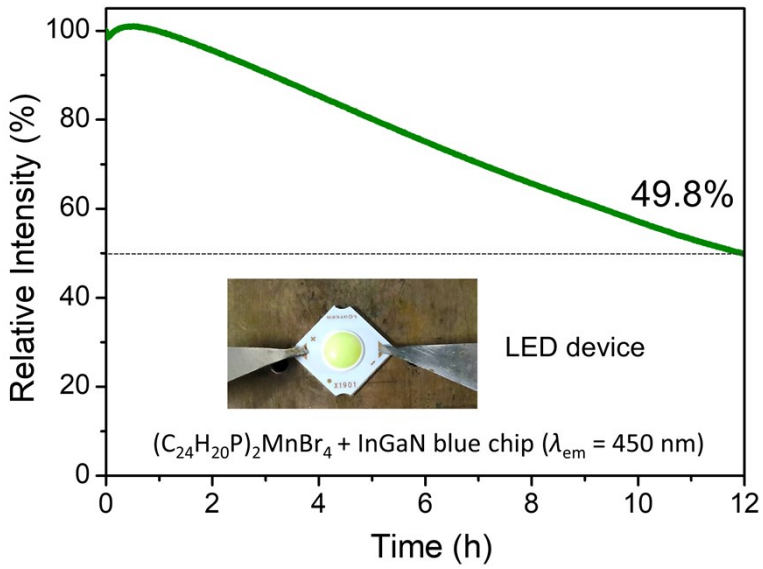

Figure. S9 Time-dependent emission intensity of the fabricated LED based on $(C_{24}H_{20}P)_2MnBr_4$ and blue chip, under 20 mA drive current for 12 h.